UvA-DARE (Digital Academic Repository)

Correlation-Driven Insulator-Metal Transition in Near-Ideal Vanadium Dioxide Films

Gray, A.X.; Jeong, J.; Aetukuri, N.P.; Granitzka, P.; Chen, Z.; Kukreja, R.; Higley, D.; Chase, T.; Reid, A.H.; Ohldag, H.; Marcus, M.A.; Scholl, A.; Young, A.T.; Doran, A.; Jenkins, C.A.; Shafer, P.; Arenholz, E.; Samant, M.G.; Parkin, S.S.P.; Dürr, H.A.

Link to publication

Citation for published version (APA):

<div align="center">

Supplemental Material for

Correlation-driven insulator-metal transition in near-ideal vanadium dioxide films

</div>

In this supplemental section we would like to present additional expanded temperature-dependent XAS and PEEM datasets detailing the results shown in the main text. These provide additional insights into the validity and interpretation of our experimental data. We also present an additional supplementary dataset for a fully-relaxed bulk-like VO_2 film, as well as some additional comments on the theoretical study cited in the letter.

Temperature- and polarization-dependent x-ray absorption (XAS) measurements – Expanded Dataset

In this supplementary section we expand on the data shown in Fig. 3a of the main text by showing individual spectra of the temperature-dependent evolution of the $d_\parallel$ V-V singlet peak, $d_\parallel$ Peierls peak, as well as the collapse of the upper band gap. These provide additional insight into the validity of our experimental data. Since all three datasets are extracted from the same XAS spectra, no temperature calibration is required to compare these two plots. The plots clearly illustrate that the two electronic-structure transitions happen at two distinct temperatures, with T_{corr}=290K and T_{IMT}=295K.
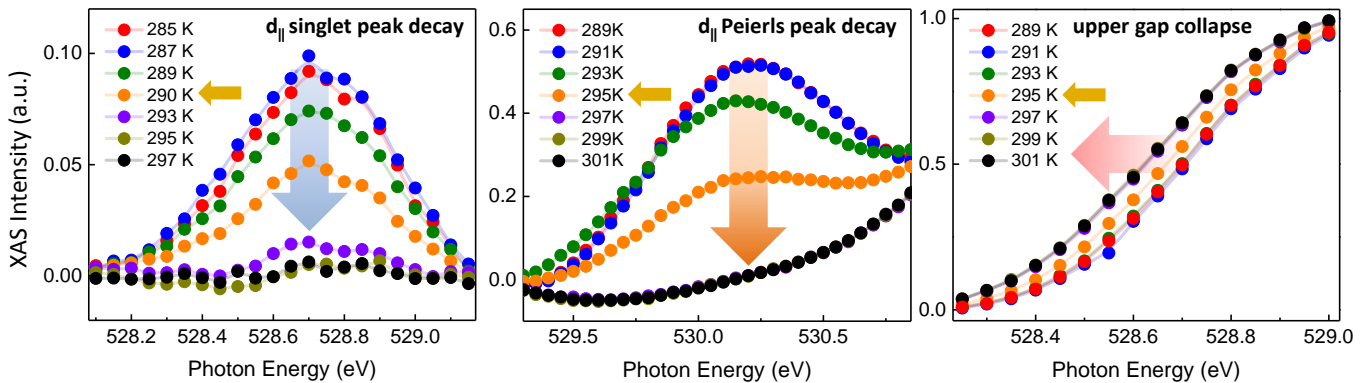

Figure S1| Two electronic transitions in VO_2 – expanded datasets. Temperature-dependent evolution of the $d_\parallel$ V-V singlet peak (left panel) showing distinctly different transition temperature (T_{corr}=290 K) as compared to the T_{IMT} (295 K), the critical temperature at which the decay of the $d_\parallel$ Peierls peak (middle panel) as well as the collapse of the upper band gap (right panel) is observed in VO_2.

Temperature-dependent PEEM measurements

In this supplementary section we address the question of spatial homogeneity of the observed phenomena since phase segregation scenarios have been observed for bulk-like and thin-film VO_2 [1-3]. A temperature- and polarization-dependent spectro-microscopic investigation of the sample using photoemission microscopy (PEEM) was carried out at the EPU beamline 11.0.1.1 of the Advanced Light Source, using the *PEEM-3* microscope routinely facilitating sub-50 nm spatial resolution.

Measurements at the leading slope of the O *K* absorption edge (528.7 eV), which is most sensitive to the collapse of the insulating gap (see Fig. S2e), reveal that our high-quality ultrathin coherently-strained VO_2 film grown in (001) crystallographic orientation on a single-crystalline TiO_2 substrate does not undergo any detectable insulator/metal phase segregation across the IMT (see Fig. S2a below). Indirectly, such quasi-instantaneous single-domain switching is evidenced by the sharpness of the transition (2-4 K width) observed in the electronic

structure via XAS (see Fig. 3a in the main text) and electronic transport measurements, as well as structurally via x-ray diffraction spectroscopy (see Fig. 1e in the main text). This is in stark contrast to a bulk-like fully-relaxed VO_2 film on $Al_2O_3(10\bar{1}0)$ substrate, which exhibits clear separation into metallic and insulating regions during the IMT at 340K (see Fig. S2b below).

Temperature-dependent PEEM measurements were carried out in 1 K steps across the IMT for both samples. Figures S2 **a** and **b** show images obtained well-below, during, and well-above the IMT as marked with yellow circles on the electronic transport curves (resistance vs temperature) in Figs. S2 **c** and **d**. As expected from the XAS spectroscopic characterization of the O K edge (Fig. S2e), metallic phase appears in the form of lighter patches at 528.7 eV for the bulk-like film (Fig. S2b). For the ultrathin film, the all-over PEEM contrast in the images of Fig. S2a follows the electronic band gap collapse in Fig. S2e without any detectable segregation into lighter (metallic) and darker (insulating) patches. All images were normalized to the beamline current, as well as the pre-edge intensity and the O K edge jump, fully-consistent with the respective XAS measurements.
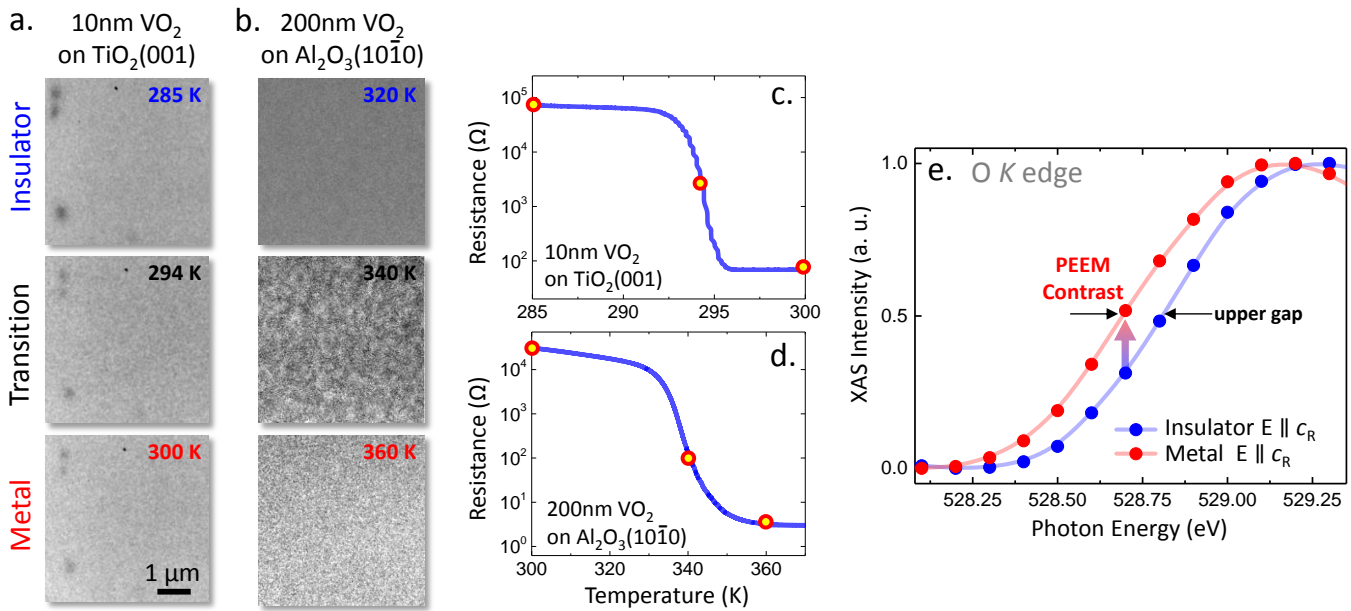

Figure S2| Temperature-dependent PEEM measurements. a. In contrast to the bulk-like VO_2 film (shown in **b**), our high-quality (near-ideal) ultrathin epitaxial VO_2 film grown on $TiO_2(001)$ substrate exhibits a homogeneous IMT without detectable phase segregation. The overall intensity of the images increases with temperature, which is consistent with the changes in the XAS intensity at 528.7 eV as VO_2 undergoes the IMT. Darker defects (specs of dust) in the left part of the images were used for fiducial alignment and focusing. **b.** Temperature-dependent PEEM images of bulk-like VO_2 film on $Al_2O_3(10\bar{1}0)$ substrate measured in the insulating state (top panel), during the IMT (middle panel) and in the high-temperature metallic state (bottom panel). Images show clear separation into metallic and insulating regions during the IMT (at 340K), in contrast with the high-quality ultrathin epitaxial VO_2 films grown on $TiO_2(001)$ substrate (shown in **a**). **c.** and **d.** Temperature-dependent electronic transport measurements (resistance vs temperature) for the two samples shown in **a** and **b**. Yellow markers indicate the temperatures (below, during and above the IMT) for the images shown in **a** and **b**. **e.** All PEEM images were obtained at the leading slope of the O K absorption edge (as measured via XAS) which is most sensitive to the collapse of the insulating gap in VO_2, and provides a clear contrast mechanism (up to 20%) between the insulating and metallic phases. XAS spectra below and above T_{IMT} such as the ones shown in **e** were measured at beamline 4.0.2 (XAS) as well as at beamline 11.0.1 (PEEM) prior to the characterization of every sample.

Temperature- and polarization-dependent x-ray absorption (XAS) measurements – comparison with a bulk-like VO₂ film

In addition to our measurements on a fully-strained VO₂(001) film on TiO₂(001) substrate, we have carried out similar polarization- and temperature-dependent XAS measurements on a fully-relaxed VO₂ film on $Al_2O_3(10\bar{1}0)$ substrate (see figure S3 below).

Our measurements suggest that the behavior we report for the ultrathin VO₂(001) film on TiO₂ substrate is ubiquitous. That is, for both fully-strained and fully-relaxed films the collapse of the gap is preceded by the softening of Coulomb correlations within V-V singlet dimers occurring at a lower temperature $T_{corr} < T_{IMT}$. As expected, in a less-then-ideal sample (VO₂ film on $Al_2O_3(10\bar{1}0)$) this effect is not as strongly pronounced as in the coherently-strained ultrathin films, mainly due to a broader and less well-defined IMT. This could also be due to phase segregation observed in this study using PEEM, as well as in prior studies with other techniques [1,2].
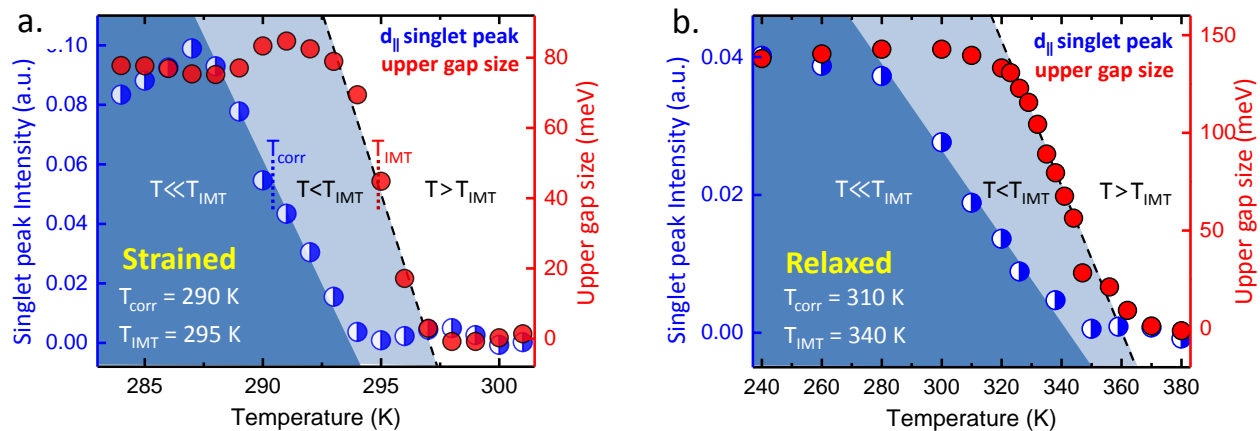

Figure S3| Temperature-dependent XAS measurements. Temperature-dependent evolution of the $d_\parallel$ V-V singlet peak intensity (blue/white symbols) for **a.** the near-ideal ultrathin coherently-strained VO₂(001) film on TiO₂ substrate, as compared to **b.** the bulk-like fully-relaxed VO₂ film on $Al_2O_3(10\bar{1}0)$ substrate. The measurements suggest that for both fully-strained and fully-relaxed films, the IMT is preceded by the purely-electronic transformation characterized by the softening of the strong correlations within the V-V dimers. For the fully-strained film in **a.** this transition occurs at $T_{corr}=290$ K (5 K below the T_{IMT}). For the fully-relaxed film in **b.** the transition is broader (consistent with the broader IMT) and is centered at $T_{corr}=310$ K (30 K below the T_{IMT}).

Additional discussion of the C-DMFT calculations by Biermann *et al.* (PRL 94, 026404, 2005)

In the theoretical study by Biermann *et al.*, state-of-the-art theoretical framework based on the cluster extension of dynamical mean-field theory (C-DMFT) in combination with density functional theory within the local density approximation (DFT-LDA) was used to effectively model the orbital-projected densities-of-states (DOS) for both rutile metallic and monoclinic insulating phases of VO₂ and to accurately predict opening of the 0.6 eV insulating band gap below the T_{IMT} [4]. Figure 1 in the main text qualitatively illustrates key aspects of the physical picture proposed in the above-mentioned theoretical model. In the high-temperature (T>T_{IMT}) metallic phase VO₂ forms rutile (*R*) lattice structure with $P4_2/mnm$ space symmetry, where V atoms occupy centers of six-fold oxygen-coordinated sites (Fig 1a in the main text). An octahedral crystal field splits the V 3*d* states, which are strongly-hybridized with the O 2*p* orbitals, into a combination of lower-lying $t2_g$ states and e_g states which lie higher in energy and are thus empty (not shown). The near-Fermi-level $t2_g$ states are furthermore

3

separated in energy by the orthorhombic component of the crystal field into the twofold-degenerate e_g^π (π*) states and a single a_{1g} orbital, which is aligned parallel to the key rutile c axis (c_R) and is thus commonly denoted $d_\parallel$. The two bands overlap in energy and the resulting non-zero density of states at the Fermi level accounts for the metallic behavior of the R phase (Fig. 1b in the main text). In the low-temperature (T<T_{IMT}) insulating phase the lattice undergoes a structural transition to a lower-symmetry ($P2_1/c$) monoclinic (M) crystal system via dimerization of the neighboring V atoms along the c_R direction and tilting of the resultant V-V dimers along the rutile [110] and [1$\bar{1}$0] directions (Fig. 1c in the main text).

The chief improvement over the prior attempts to self-consistently describe the metallic and insulating phases within one theoretical framework is achieved by modeling the monoclinic state as a molecular solid wherein the key building block is a strongly-correlated dynamical V-V singlet dimer (Fig. 1c in the main text). Within this picture, the two V $3d^1$ electrons form a singlet state on each dimer, and can be shared between the dimers via the self-consistent electronic bath. Consistent with the prior models [5-7], C-DMFT predicts that the c_R dimerization will split the highly-directional $d_\parallel$ orbitals into the bonding and anti-bonding bands and that the tilting of the dimers will shift the π* band to higher energies due to the increase of the p-d orbital overlap. However, in contrast with the conventional methods, this cluster-extended approach also succeeds in producing an insulating gap of 0.6 eV – the key aspect of the monoclinic phase observed via a wide variety of experimental techniques but absent or mischaracterized in prior theoretical calculations. The model also correctly predicts changes in the V $3d$ orbital occupation from almost isotropic in the metallic phase to almost completely (~81%) $d_\parallel$-polarized in the insulating state, consistent with the recent experimental observations via polarization-dependent XAS [8,9].

Strong Coulomb correlations within dynamical V-V singlet dimers in the insulating phase give rise to distinct additional DOS spectral features both above and below the Fermi level [4]. For the occupied valence-band manifold, presence of the additional coherent quasiparticle peak at ~0.9 eV below the E_F has been recently confirmed with both soft x-ray [10] and bulk-sensitive hard x-ray [11] photoemission spectroscopies. On the other hand, above the Fermi level, these correlations are manifested by a small but detectable amount of $d_\parallel$ orbital character in the form of a sharp peak at the very onset of the unoccupied conduction band (dimer V-V singlet state), which is accessible experimentally via polarization-dependent XAS at the oxygen (O) K edge (Ref. 10 and this work). This spectral feature arises as a direct consequence of the formation of the strongly-correlated dynamical V-V dimer state within the theoretical cluster picture. It is unique to the C-DMFT description of the insulating state on VO$_2$, and thus presents a distinct signature of the strong Coulomb correlations within the dynamical V-V singlet dimers [4,10].

Error bar analysis

In this supplementary section we show the results of the error bar analysis for the parameters plotted in Figure 3a of the main paper. Both dichroism peaks – the $d_\parallel$ V-V singlet peak as well as the $d_\parallel$ V-V Peierls peak were fitted with single-peak Gaussian functions. Error in the measured intensity due to the uncertainty of the fit does not exceed ±3% of the maximum intensity for either peak. Thus, the error bars (shown in Fig. S4 below) are smaller than the size of the symbols (circles) used to plot the data. The edge threshold was fitted using a 4th-order polynomial function. Resultant error in the value of the upper gap size due to the uncertainty of the fit does not exceed ±7 meV, corresponding to ±8.3% of the maximum upper gap value. The error bars are shown in Fig. S4 below.

Energy stability of the beamline has been evaluated and for the mode of operation used in this study amounts to less than 1 meV uncertainty, which is negligible compared to the size of the upper band gap (~80 meV). Uncertainty in the intensity is autocorrected for by continuous automatic normalization by x-ray beam current, measured via a gold mesh

upstream from the analysis chamber. Uncertainty in the polarization angle of the x-rays is determined by the stability of the magnetic field in the undulator and is negligible for vertical/horizontal linear polarization.
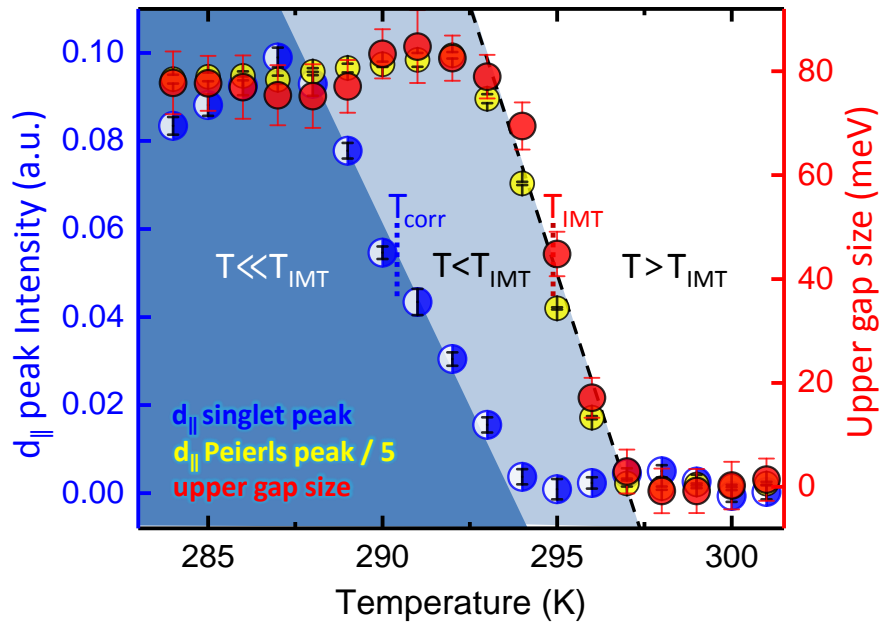

Figure S4| Error bar analysis for the parameters plotted in Figure 3a of the main paper. Error in the measured intensities of the $d_\parallel$ V-V singlet peak (blue/white circles) as well as the $d_\parallel$ V-V Peierls peak (yellow circles) does not exceed $\pm 3\%$ of the maximum intensity for either peak. Error in the value of the upper gap size (red circles) due to the uncertainty of the fit does not exceed ± 7 meV.

Temperature-dependent x-ray diffraction measurements – Expanded Dataset

In this supplementary section we expand on the data shown in Fig. 1e of the main text by showing individual θ-2θ scans across the IMT.
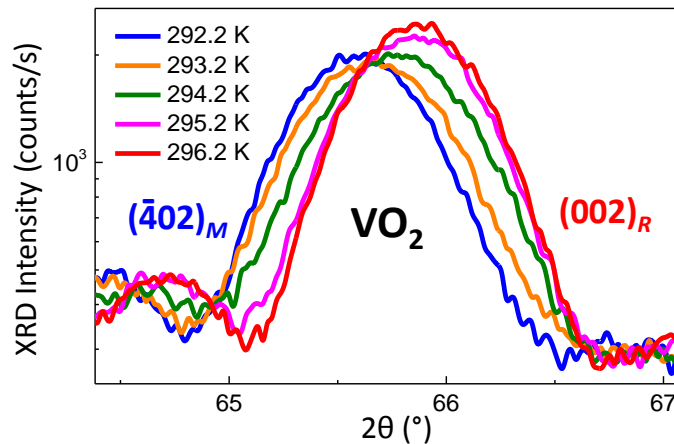

Figure S5| Temperature-dependent x-ray diffraction measurements. Temperature-dependent x-ray diffraction θ-2θ scans across the VO₂ film peaks show a clear structural transition in VO₂ manifested by an abrupt change in the inter-planar atomic spacing along the direction normal to the film surface (see Fig. 1e in the main letter).

References

1. M. M. Qazilbash *et al.*, Science **318**, 1750 (2007).
2. M. M. Qazilbash *et al.*, Phys. Rev. B **83**, 165108 (2001).
3. M. K. Liu *et al.*, Phys. Rev. Lett. **111**, 096602 (2013).
4. S. Biermann *et al.*, Phys. Rev. Lett. **94**, 026404 (2005).
5. J. B. Goodenough, J. Solid State. Chem. **3**, 490 (1971).
6. R. M. Wentzcovitch, W. Schulz, and P. Allen, Phys. Rev. Lett. **72**, 3389 (1994).
7. V. Eyert, Ann. Phys. (Leipzig) **11**, 648 (2002).
8. N. B. Aetukuri *et al.*, Nature Physics **9**, 661 (2013).
9. M. W. Haverkort *et al.*, Phys. Rev. Lett. **95**, 196404 (2005).
10. T. C. Koethe *et al.*, Phys. Rev. Lett. **97**, 116402 (2006).
11. S. Suga *et al.*, New J. Phys. **11**, 103015 (2009).